

GrokFormer: Graph Fourier Kolmogorov-Arnold Transformers

Guoguo Ai¹, Guansong Pang², Hezhe Qiao², Yuan Gao¹, Hui Yan^{1*}

¹School of Computer Science and Engineering

Nanjing University of Science and Technology, Nanjing, China

Email: {guoguo, maxgaoyuan, yanhui}@njust.edu.cn

²School of Computing and Information Systems, Singapore Management University, Singapore

Email: gspang@smu.edu.sg, hezheqiao.2022@phdcs.smu.edu.sg

arXiv:2411.17296v1 [cs.LG] 26 Nov 2024

Abstract—Graph Transformers (GTs) have demonstrated remarkable performance in incorporating various graph structure information, *e.g.*, long-range structural dependency, into graph representation learning. However, self-attention – the core module of GTs – preserves only *low-frequency signals* on graph features, retaining only *homophilic patterns* that capture similar features among the connected nodes. Consequently, it has insufficient capacity in modeling complex node label patterns, such as the opposite of homophilic patterns – *heterophilic patterns*. Some improved GTs deal with the problem by learning polynomial filters or performing self-attention over the first-order graph spectrum. However, these GTs either ignore rich information contained in the whole spectrum or neglect higher-order spectrum information, resulting in limited flexibility and frequency response in their spectral filters. To tackle these challenges, we propose a novel GT network, namely **Graph Fourier Kolmogorov-Arnold Transformers (GrokFormer)**, to go beyond the self-attention in GTs. GrokFormer leverages learnable activation functions in order- K graph spectrum through Fourier series modeling to i) learn eigenvalue-targeted filter functions producing learnable base that can capture a broad range of frequency signals flexibly, and ii) extract first- and higher-order graph spectral information adaptively. In doing so, GrokFormer can effectively capture intricate patterns hidden across different orders and levels of frequency signals, learning *expressive, order-and-frequency-adaptive graph representations*. Comprehensive experiments conducted on 10 node classification datasets across various domains, scales, and levels of graph heterophily, as well as 5 graph classification datasets, demonstrate that GrokFormer outperforms state-of-the-art GTs and other advanced graph neural networks. Our code is available at <https://github.com/GGA23/GrokFormer>.

Index Terms—Graph Transformers, Graph Neural Networks, Graph Spectral Filters, Fourier, Kolmogorov-Arnold Networks, Graph Representation Learning.

I. INTRODUCTION

Transformers [1] have proved to be successful in numerous domains, such as natural language understanding [1] and computer vision [2]. One key advantage of transformers is that a single self-attention layer in the Transformer networks can capture interactions between any pair of input instances, *e.g.*, graph nodes, enabling the direct modeling of long-range relationships. This capability has led researchers to explore ways to adapt the Transformer architecture for graph representation learning that captures long-range dependencies.

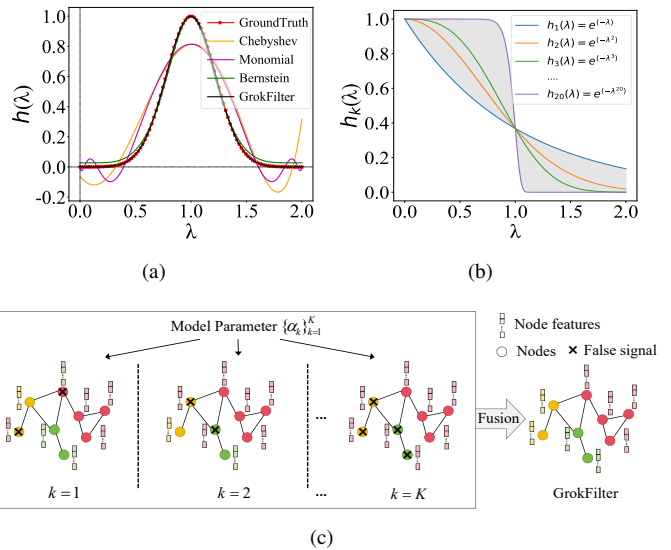


Fig. 1: (a) Band-pass filter (ground truth) and the approximated filters generated by the filter learning module in our GrokFormer (GrokFilter) and three popular polynomial functions: Chebyshev, Monomial, and Bernstein. (b) Frequency response curve of existing low-pass filters $h_k(\lambda)$ at the spectrum λ with an order k against that of our GrokFilter which can adaptively capture diverse frequency response covered by the full shaded area. (c) A toy example showing the ability of the low-pass filters in (b) in capturing different levels of frequency signals on a graph where eight nodes are divided into three classes, each marked with a different color. When $k=1$, $h_1(\lambda)$ preserves some low- and high-frequency graph signals; when $k=2$, $h_2(\lambda)$ preserves more low-frequency and suppress more high-frequency signals than $k=1$; and when $k=K$ being large enough, the low-pass filter $h_K(\lambda)$ only retains the low-frequency signal, modeling strong homophily. These individual filters $h_k(\lambda)$ can be adaptively fused by a learnable parameter α_k in our GrokFilter to accurately model varying levels of homophily on the graph.

Several Graph Transformers (GTs) are proposed by intro-

ducing position encoding techniques based on modules like Laplacian vectors and random walks to integrate topological structure information into the Transformers [3]–[7]. Beyond graph topological structure, additional information such as graph distances, path embeddings, and node representations can also be flexibly incorporated into GTs via its attention mechanism [8]–[12].

While GTs can be effectively applied to graph representation learning on networks with strong *homophily* where most connected nodes share similar features or the same class label, such as citation networks, they often lack competitiveness in downstream tasks, particularly in node-level tasks like node classification [13]. This limitation arises mainly from the inherently low-pass nature of self-attention [14]–[16], since low-pass filters are focused on smoothing operation across nodes which retain primarily *low-frequency signals* that highlight similar features among nodes, whereas many real-world graph learning tasks exhibit varying label distribution patterns, *e.g.*, homophilic and heterophilic (see Table II in Sec. V), on which going beyond low-frequency modeling is required to gain the desired accuracy [17], [18]. For example, in dating networks, the majority of people tend to connect with people of the opposite gender, leading to networks with strong *heterophily* where the most connected nodes belong to different classes [19]. In this scenario, *high-frequency signals* that highlight these differences between nodes can be particularly valuable. Therefore, the key question we ask here is: *can we have a GT that has the capability of extracting varying levels of frequency signals from graphs with different homophily-heterophily properties flexibly?*

There have been some attempts recently to solve this problem. Inspired by spectral Graph Neural Networks (GNNs) [17], [18], [20], [21], one line of research is dedicated to capturing various frequency signals by learning polynomial spectral filters [14], [22], [23]. The underlying key idea is that, by relying on the diagonalization of symmetric matrices, polynomial filters avoid direct spectral decomposition and can be applied uniformly across all eigenvalues. However, this approach leads to a loss of the rich spectral information contained in each individual eigenvalue. Moreover, these polynomial functions mostly are linear and truncated, have a limited learning capabilities. As shown in Fig. 1(a) where we employ the band-pass filter function that maps the spectrum of the symmetric normalized Laplacian $\lambda \in [0, 2]$ to $h(\lambda)$ [17], *i.e.*, $h(\lambda) = e^{-10(\lambda-1)^2}$, as the ground truth to test the learning ability of three polynomial functions of varying capacity. It is clear that these polynomials failed to accurately fit this band-pass filter function, demonstrating their limited learning ability to capture complex frequency responses (see more results in Sec. V-C1).

Another approach tackles the problem by treating each eigenvalue of the first-order graph Laplacian as an independent token for self-attention [13]. While this approach shows impressive effectiveness, it still misses some valuable frequency components embedded in different order graph spectrum. To demonstrate this, we take low-pass filter defined

as $h(\lambda) = e^{(-\lambda)}$ [24] as an example and show, from both the spectral and spatial domains, that using spectral filters of a fixed order k have limited capability of modeling different levels of homophily, as shown in Figs. 1(b)(c). For example, the low-pass filter of a small order k preserves some low- and high-frequency signals, while the higher-order filter captures low-frequency signals much better yet substantially suppresses high-frequency signals. Therefore, it is crucial to learn multi-order spectral filters, rather than relying solely on a fixed-order filter, for effectively modeling complex network homophily.

To address the aforementioned limitations, we develop a novel GT network, called Graph Fourier Kolmogorov-Arnold Transformers (GrokFormer), which effectively capture intricate frequency components hidden across different order graph spectrum, learning *expressive, order-and-frequency-adaptive graph representations* to go beyond the self-attention in GTs. Specifically, GrokFormer leverages learnable activation functions modeled as Fourier series in the spectral domain to efficiently learn the eigenvalue-targeted filter function from the first-order to K -order graph spectrum. The spectral property of the Fourier series enable the model to capture various frequency components, and the activation functions with learnable Fourier coefficients give the GrokFormer a powerful ability to flexibly adjusts the importance of different frequency components. Accordingly, our GrokFormer can adaptively extract non-linearity and intricate frequency response embedded across the entire spectrum, offering significantly greater expressiveness than linear polynomials in learning complex filters (see Fig. 1(a)). As a result, our GrokFormer can incorporate effective order information adaptively by introducing learnable parameter to capture signals at different frequency levels, thereby facilitating the modeling of various levels of homophily in graphs, as illustrated in Figs. 1(b)(c). In doing so, GrokFormer protects global long-range dependencies while efficiently and adaptively capturing a broad range of frequency signal across K -order graph spectrum. The flexible and rich frequency response helps learn high-quality, more expressive graph representations.

Our key contributions are summarized as follows:

- We design a novel eigenvalue-targeted efficient filter learning method, which leverages learnable activation functions modeled as Fourier series flexibly extract non-linearity and various levels of frequency signals from a broad graph spectrum from the first to K -th orders.
- We further propose GrokFormer, a novel GT model, for graph representation learning. It preserves global long-range dependencies in the spatial domain while effectively modeling various levels of homophily in the spectral domain.
- Extensive experiments on 10 node classification benchmark datasets across various domains, scales, and levels of graph heterophily, as well as 5 graph classification datasets reveal the superior performance of GrokFormer in graph representation learning, consistently outperforming a number of state-of-the-art GTs and GNNs.

II. RELATED WORK

Graph Neural Networks. Existing GNNs are mainly divided into two main streams: spatial-based and spectral-based methods. Spatial-based GNNs, like GCN [25] and GAT [26], update node representations by aggregating information from first-order neighbors. By stacking multiple layers, they may learn long-range dependencies but suffer from over-smoothing [27] and over-squashing [28]. Besides, the smooth nature of their aggregation mechanism prevents them from being successfully applied to heterophilic scenarios. To this end, some spatial-based methods, such as H2GCN [29] and HopGNN [30], propose to combine first-order and higher-order neighborhood representations. Other studies [24], [31] point out from a spectral perspective that GCN only considers the first-order Chebyshev polynomial, which acts as a low-pass filter. As a result, various spectral-based GNNs have been proposed to leverage different types of polynomials to approximate arbitrary filters. For instance, GPR-GNN [18] employs the Monomial basis for graph filter approximation. ChebyNet [20] proposes a fast localized convolutional filter based on Chebyshev polynomial. APPNP [32] utilizes Personalized PageRank (PPR) to achieve a low-pass filter. BernNet [17] learns arbitrary graph spectral filters by an order- K Bernstein polynomial approximation. JacobiConv [21] approximates filter functions with Jacobi basis. HiGCN [33] incorporates Flower-Petals Laplacians into simplicial complexes, capable of learning graph filters across varying topological scales. However, these pre-defined linear polynomial filters usually have limited learning ability.

Graph Transformers. Compared to GNNs, the attention weights learned by Transformers can be seen as a weighted adjacency matrix of a fully connected graph, which is advantageous to learn long-range dependency of the graph nodes [34]. However, the primary transformers lack structural topology information. Therefore, graph transformers (GTs) are proposed by incorporating graph structural information into the Transformer architecture via various ways. For example, GT [4] leverages eigenvectors of graph Laplacian matrix as part of the input features to encode the local structure information. SAN [5] leverages the full spectrum of the Laplacian matrix to learn the positional encodings. GraphTrans [7], GPS [35], SAT [10] and SGFormer [12] combine GNN and Transformers with GNN model used as the structure extractor to capture local structural information. Graphormer [9], NodeFormer [36], and EGT [37] transform various graph structure features into attention biases, allowing the Transformer to capture graph structural information. However, all these GTs rely on the attention matrix to learn node representations, which has been proven as a smoothing operation on all nodes, capturing only the low-frequency information of graph features [14]. This is insufficient to extract complex label distributions resulting from a mixture of low- and high-frequency information [38].

Recently, advanced GTs have increasingly focused on capturing various frequency signals to enhance the performance [14], [22], [39]. SignGT [39] designs a new signed self-

attention mechanism to capture low-frequency and high-frequency information. FeTA [14] learns polynomial filters using the self-attention weights. PolyFormer [22] performs self-attention on polynomial tokens to protect the rich frequency information. Specformer [13] parameterizes the spectral filters by performing self-attention on N eigenvalue tokens of the first-order graph Laplacian. Although these improved GTs capture different frequency signals on graph features, they still struggle to derive the desired frequency response hidden at varying order graph spectrum.

III. PRELIMINARIES

In this section, we first briefly introduce notations and the problem definition, then introduce the graph signal filter in the spectral domain. Finally, we introduce the key module self-attention of Transformer architecture and Kolmogorov-Arnold Network.

A. Notations and the Problem

An undirected, unweighted attributed graph is represented as $\mathcal{G} = (\mathcal{V}, \mathcal{E}, \mathbf{X})$, where \mathcal{V} denotes the node set with $v_i \in \mathcal{V}$ and $|\mathcal{V}| = N$, \mathcal{E} denotes the edge set, and $\mathbf{X} = [x_1, x_2, \dots, x_N] \in \mathbb{R}^{N \times F}$ is a set of node attributes (features). Each node v_i has a F -dimensional feature representation x_i . The topological structure of \mathcal{G} is represented by an adjacency matrix $\mathbf{A} = [a_{ij}] \in \mathbb{R}^{N \times N}$, $a_{ij} = a_{ji} = 1$ if $(v_i, v_j) \in \mathcal{E}$, or 0 otherwise. $\mathbf{D} \in \mathbb{R}^{N \times N}$ denotes a degree matrix which is a diagonal matrix with $d_{ii} = \sum_j a_{ij}$. Normalized Laplacian matrix \mathbf{L} is defined by $\mathbf{L} = \mathbf{I}_N - \mathbf{D}^{-\frac{1}{2}} \mathbf{A} \mathbf{D}^{-\frac{1}{2}}$, where $\mathbf{I}_N \in \mathbb{R}^{N \times N}$ denotes an identity matrix.

The homophily ratio \mathcal{H} as a measure of the graph homophily level is used to define graphs with strong homophily/heterophily. The mathematical expression for the homophily ratio is $\mathcal{H} = \frac{|\{(v_i, v_j) \in \mathcal{E} \wedge y_i = y_j\}|}{|\mathcal{E}|}$ [29], which is the fraction of edges in a graph which connect nodes that have the same class label. Homophily ratio $\mathcal{H} \rightarrow 1$ represents the graph exhibit strong homophily, while the graph with strong heterophily (or low/weak homophily) have small homophily ratio $\mathcal{H} \rightarrow 0$.

Each node v_i contains a unique class label y_i . The goal of semi-supervised node classification is to learn a mapping $\mathcal{M}_n : \mathcal{V} \rightarrow \mathcal{Y}$, where \mathcal{Y} is the set of labels, given a set of labeled node $\mathcal{V}_L = \{(v_1, y_1), (v_2, y_2), \dots, (v_t, y_t)\}$ as training data. Similarly, the goal of the graph classification is to find a mapping $\mathcal{M}_g : \mathcal{G} \rightarrow \mathcal{Y}$, given a set of graphs $\mathcal{G} = \{G_1, \dots, G_t\}$ and a set of labels $\mathcal{Y} = \{y_1, \dots, y_t\}$ as training data.

B. Graph Signal Filter

Suppose that Laplacian matrix \mathbf{L} is the graph shift operator that respects the graph topology. The eigendecomposition of Laplacian matrix is $\mathbf{L} = \mathbf{U} \mathbf{\Lambda} \mathbf{U}^\top$, where $\mathbf{U} = (u_1, u_2, \dots, u_N)$ is a complete set of orthonormal eigenvectors known as graph Fourier modes and $\mathbf{\Lambda} = \text{diag}(\{\lambda_i\}_{i=1}^N)$ is a diagonal matrix of the eigenvalues of \mathbf{L} . The i^{th} column of \mathbf{U} satisfies $\mathbf{L}u_i = \lambda_i u_i$.

TABLE I: The filter form of different spectral GNNs

Model	Filter
GCN	$h(\lambda) = (1 - \lambda)^k$
ChebyNet	$h_k(\lambda) = 2\lambda h_{k-1}(\lambda) - h_{k-2}(\lambda), h_0(\lambda) = 1, h_1(\lambda) = \lambda$
APPNP	$h(\lambda) = \sum_{k=0}^K \frac{\gamma_k}{1-\gamma} (1-\lambda)^k$
GPR-GNN	$h(\lambda) = \sum_{k=0}^K \gamma_k (1-\lambda)^k$
BernNet	$h(\lambda) = \sum_{k=0}^K \alpha_k \binom{K}{k} (1 - \frac{\lambda}{2})^{K-k} (\frac{\lambda}{2})^k$
JacobiConv	$h(\lambda) = \sum_{k=0}^K \alpha_k \sum_{s=0}^k \frac{(k+a)!(k+b)!(-\lambda)^{k-s}(2-\lambda)^s}{2^k s!(k+a-s)!(b+s)!(k-s)!}$
HiGCN	$h(\lambda) = \sum_{k=0}^K \gamma_{p,k} (1 - \lambda_p)^k, p = 1, 2, \dots, P$

The graph Fourier transform of a graph signal $\mathbf{X} \in \mathbb{R}^{N \times F}$ is written as $\hat{\mathbf{X}} = \mathbf{U}^\top \mathbf{X}$. The inverse transform is $\mathbf{X} = \mathbf{U} \hat{\mathbf{X}}$ [40]. $\hat{\mathbf{X}}_i = u_i^\top \mathbf{X}$, is the frequency component of \mathbf{X} at λ_i frequency. In other words, u_i is a frequency component corresponding to the eigenvalue λ_i . If $\hat{\mathbf{X}}_i \neq \vec{0}$, it means \mathbf{X} contains the λ_i frequency component. Otherwise, the λ_i frequency component is missing from \mathbf{X} .

According to the convolution theorem, the convolution of the graph signal \mathbf{X} with a spectral filter G having its frequency response as h is obtained by:

$$\mathbf{X} * G = \mathbf{U} h(\Lambda) \mathbf{U}^\top \mathbf{X} = \mathbf{U} \text{diag}[h(\lambda_1), \dots, h(\lambda_N)] \mathbf{U}^\top \mathbf{X}, \quad (1)$$

where $h(\Lambda)$ applied h element-wisely to the diagonal entries of Λ , i.e., $[h(\Lambda)]_{ii} = h(\lambda_i)$. A powerful spectral filter can exploit useful frequency components on graphs. In Table I, we show the polynomial filter form of some popular spectral GNNs: GCN [25], ChebyNet [20], APPNP [32], GPR-GNN [18], BernNet [17], JacobiConv [21], and HiGCN [33]. Relying on the diagonalization of symmetric matrices, these polynomial filters avoid direct spectral decomposition and can be applied uniformly across all eigenvalues, i.e., $h(\lambda) = h(\mathbf{L})$, inevitably ignoring the spectral information embedded in each eigenvalue.

C. Self-Attention

The multi-head self-attention is the critical module of Transformers and has garnered substantial attention due to their capacity for point-to-point feature interactions within item sequences. Let $\mathbf{X} \in \mathbb{R}^{N \times F}$ denote the input of the self-attention, for simplicity of illustration, we consider the single-head self-attention for description. It first projects \mathbf{X} into three subspaces \mathbf{Q} , \mathbf{K} , \mathbf{V} through three projection matrices $\mathbf{W}^Q, \mathbf{W}^K, \mathbf{W}^V$:

$$\mathbf{Q} = \mathbf{X} \mathbf{W}^Q, \quad \mathbf{K} = \mathbf{X} \mathbf{W}^K, \quad \mathbf{V} = \mathbf{X} \mathbf{W}^V. \quad (2)$$

The self-attention is then calculated as:

$$\text{Attention}(\mathbf{Q}, \mathbf{K}, \mathbf{V}) = \text{softmax}\left(\frac{\mathbf{Q} \mathbf{K}^\top}{\sqrt{d}}\right) \mathbf{V}. \quad (3)$$

The attention weights capture the pair-wise similarity of input items in the sequences. This mechanism effectively addresses the challenge of global dependencies and enables the incorporation of longer sequences enriched with a wealth of information.

However, self-attention has one critical difficulty, i.e., the scalability issue with $\mathcal{O}(N^2)$ computational complexity, which is prohibitive for large networks. To reduce the algorithmic complexity of self-attention, one of efficient attention switches the order from $(\mathbf{Q} \mathbf{K}^\top) \mathbf{V}$ to $\mathbf{Q} (\mathbf{K}^\top \mathbf{V})$ [41], which no impact on the effect but changes the complexities from $\mathcal{O}(N^2 d)$ to $\mathcal{O}(N d^2)$, where d is hidden dimension and $d \ll N$.

D. Kolmogorov-Arnold Network

The KAN offers a promising alternative to Multi-Layer Perceptron (MLP). While MLP is based on the universal approximation theorem [42], KAN is grounded in the Kolmogorov-Arnold representation theorem [43]. The fundamental idea of KAN is to create an arbitrary function at each hidden neuron by overlaying multiple nonlinear functions onto the input features. It can be expressed in the following formula:

$$\text{KAN} = f(x) = \sum_{q=1}^{2n+1} \Phi_q \left(\sum_{p=1}^n \phi_{q,p}(x_p) \right), \quad (4)$$

where $\phi_{q,p}$ is trainable activation function, and $\Phi_q: [0,1] \rightarrow \mathbb{R}$ and $\phi_{q,p}: \mathbb{R} \rightarrow \mathbb{R}$ are univariate functions that map each input variable x_p . In the Kolmogorov-Arnold theorem, the inner functions form a KAN layer with $n_{in} = n$ and $n_{out} = 2n + 1$, and the outer functions form a KAN layer with $n_{in} = 2n + 1$ and $n_{out} = n$. Thus, the Kolmogorov-Arnold representations in this formula are simply compositions of two KAN layers. A useful trick is that it includes a basis function $b(x)$ such that the activation function $\phi(x)$ is the sum of the basis function $b(x)$ and the spline function:

$$\phi(x) = w_b b(x) + w_s \text{spline}(x), \quad b(x) = \text{silu}(x) = \frac{x}{1 + e^{-x}}, \quad (5)$$

where $\text{spline}(x)$ is parametrized as a linear combination of B-splines in most cases. It can be expressed as follows:

$$\text{spline}(x) = \sum_i c_i B_i(x), \quad (6)$$

where c_i is trainable.

IV. METHODOLOGY

A. Overview of the Proposed GrokFormer

Our new approach falls into the framework of Transformer with a Graph Fourier Kolmogorov-Arnold Network being added as a new spectral graph convolutional module, as shown in Fig. 2, so we named it as Graph Fourier Kolmogorov-Arnold Transformers (GrokFormer). The central piece of the GrokFormer is a order-and-frequency-adaptive convolution module designed to extract diverse frequency information, going beyond the self-attention mechanism, to model varying levels of graph homophily. Specifically, we first leverage learnable activation functions modeled as Fourier series to learn eigenvalue-targeted filter function from K order graph spectrum. After that, K spectral filters from the first order to the K -th order are adaptively fused to produces the learnable filter base for conducting graph convolution. Finally, the information from the self-attention mechanism and spectral

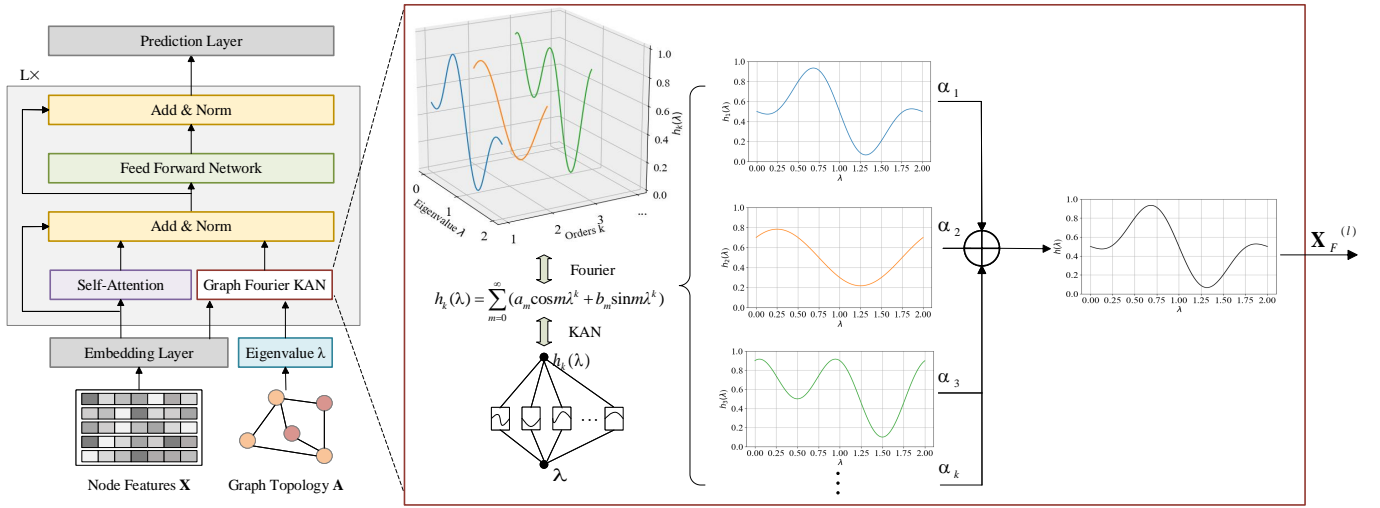


Fig. 2: The framework of the proposed GrokFormer. The feature matrix \mathbf{X} is first fed into the embedding layer and the spectral decomposition is pre-processed. Then, the multi-head self-attention module and the Graph Fourier KAN extract the global graph information and the desired frequency response across K order graph spectrum, respectively. Finally, as all Transformers do, the information from two modules is fused by a summation and normalization layer, and subsequently a Feed-Forward Network (FFN) layer for prediction.

graph convolution is merged to output the final representation for prediction.

B. Order-and-frequency-adaptive Graph Filter

To capture various frequency details in a flexible and fine-grained manner from the K order graph spectrum, we design a novel spectral graph convolution module. Motivated by the Kolmogorov-Arnold representation theorem [43] and Kolmogorov-Arnold Network (KAN) that involves a network design where traditional weight parameters are substituted with learnable activation functions, we develop Graph Fourier KAN, which utilizes learnable activation functions modeled as the Fourier series to learn eigenvalue-target frequency adaptive filter function. This approach allows for adaptively capturing global and a broad range of frequency components. Specifically, we leverage Fourier series representation [44] to parameterize each learnable function since the spline functions in KAN are piecewise and difficult to train. The specific filter learning is can be defined as follows:

$$\phi_h(\lambda) = \sum_{k=1}^K \sum_{m=0}^M (\cos(m\lambda^k) \cdot a_{km} + \sin(m\lambda^k) \cdot b_{km}), \quad (7)$$

where k is the order. a_{km} and b_{km} are trainable Fourier coefficients. The hyperparameter m represents the number of frequency components (or grid size) and can be fine-tuned. The spectral properties of the Fourier series, which represent different frequency components, enable the model to control and achieve a broad range of frequency responses. Furthermore, trainable Fourier coefficients empower the model to adaptively capture the various frequency information.

The benefits of $\phi_h(\lambda)$ are five-fold: (i) efficiency. Compared to spline functions or performing self-attention over N eigenvalues, which has a complexity of $\mathcal{O}(N^2)$, Fourier series representation has a lower training complexity, with a linear complexity of $\mathcal{O}(N)$. (ii) Effectiveness. Sine and cosine in the Fourier series are orthogonality. Orthogonal basis have been shown to enable more effective learning of graph filters [21]. (iii) Informative. Many sine and cosine terms with different frequency components can capture rich frequency responses in different graph spectral spaces. (iv) Convergence guarantee. In approximation theory, it is well established that the Fourier series attains the best convergence rate for function approximation. (v) Globality. The filter function pay attention to the whole spectrum (all eigenvalues), capturing the global information [13].

Previous work focuses on learning graph filters solely from the eigenvalues derived from the first-order graph Laplacian, which inevitably overlooks higher-order spectral information. To address this limitation, we consider the K -order graph spectrum in this work. Furthermore, to adaptively capture diverse patterns across different orders, we first learn filtering functions for each order separately. Thus, we can rewrite Eq. (7) as follows:

$$h_k(\lambda) = \sum_{m=0}^M (\cos(m\lambda^k) \cdot a_m + \sin(m\lambda^k) \cdot b_m), \quad (8)$$

where $k = [1, 2, \dots, K]$. Furthermore, to achieve order-adaptive filter function, we learn a free parameter α to adaptively fusing varying order's filter as follows,

$$h(\lambda) = \sum_k^K \alpha_k h_k(\lambda). \quad (9)$$

Therefore, the corresponding spectral graph convolution in GrokFormer is as follows,

$$\mathbf{X}_F^{(l)} = \mathbf{U} \text{diag}(h(\lambda)) \mathbf{U}^\top \mathbf{X}^{(l-1)}, \quad (10)$$

where $\text{diag}(\cdot)$ is a function that creates a diagonal matrix. $\mathbf{X}^{(0)} = f_\theta(\mathbf{X})$, and f_θ is a two-layer MLP (embedding layer). $\mathbf{U} \text{diag}(h(\lambda)) \mathbf{U}^\top$ is the filter base, similar to the purpose of those polynomial bases in the literature. In doing so, GrokFormer achieves eigenvalue-target order-and-frequency-adaptive graph filter capturing desired frequency response tailored to varying network properties.

C. Network Architecture of GrokFormer

GrokFormer is built upon the original implementation of a classic Transformer encoder. Specifically, we first apply layer normalization (LN) on the representations before feeding them into other sub-layers, i.e., the multi-head self-attention (MHA) and the feed-forward blocks (FFN). The LN trick has been used widely to improve the optimization of Transformer [9]. Then, we combine the information from self-attention block and the Graph Fourier KAN through summation to generate informative node representations. We formally characterize the GrokFormer layer as follows:

$$\begin{aligned} \mathbf{X}'^{(l)} &= \text{MHA}(\text{LN}(\mathbf{X}^{(l-1)})) + \mathbf{X}^{(l-1)} + \mathbf{X}_F^{(l)}, \\ \mathbf{X}^{(l)} &= \text{FFN}(\text{LN}(\mathbf{X}'^{(l)})) + \mathbf{X}'^{(l)}. \end{aligned} \quad (11)$$

In the final layer of GrokFormer, we calculate the prediction scores of the nodes from class c . This score is given by:

$$\hat{\mathbf{Y}} = \text{softmax}(\mathbf{X}^{(L)}), \quad (12)$$

where $\mathbf{X}^{(L)}$ is the output of the final layer, and $\hat{\mathbf{Y}}$ is the predicted class label.

Then, GrokFormer can be trained by minimizing the cross entropy between the predicted and the (partial) ground-truth labels:

$$\mathcal{L}_{ce} = - \sum_{i \in \mathcal{V}_L} \sum_{c=1}^C \mathcal{Y}_{ic} \ln \hat{\mathbf{Y}}_{ic}, \quad (13)$$

where C is the number of classes, \mathcal{Y} is the real labels, and \mathcal{V}_L is the training set.

D. Complexity and Scalability Analysis

Complexity. Firstly, like some previous methods, such as NAGphormer [45], Specformer [13] and Sp²GCL [46], GrokFormer also needs spectral decomposition, which is preprocessing and has the complexity of $O(N^3)$. Secondly, GrokFormer has another part of the computation, i.e., the forward process. The forward complexity of GrokFormer includes efficient self-attention, filter base learning, and graph convolution. Their corresponding complexities are $O(Nd^2)$, $O(KNM)$, and $O(N^2d)$, respectively, where d denotes the hidden dimension, N represents the number of nodes, M is the number of terms used in the Fourier series expansion, and K is the order. The overall forward complexity is $O(Nd(N+d) + KNM)$.

Scalability. In the context of large graphs, the complexity of decomposition is unacceptable. Therefore, we employ Sparse Generalized Eigenvalue (SGE) algorithms, as outlined in earlier studies [13], [47], to compute q eigenvalues and corresponding eigenvectors, which reduces the complexity to $O(N^2q)$ [46]. Accordingly, the complexity of graph convolution reduce to $O(q^2d)$, thus the forward complexity reduce to $O(Nd^2 + KNM + q^2d)$, $q \ll N$, which is linear in the number of nodes. Note that the decomposition is only computed once, thus the overhead of the preprocessing should be amortized by each training epoch (see Sec. V-A for empirical results).

E. Remarks on the Advantages of GrokFormer

Comparison to Spectral GNNs. Most spectral GNNs design linear polynomial spectral filters, as shown in Table I. In contrast, our GrokFormer has the following advantages: (1) globality. On the one hand, the transformer architecture enables our model to capture long-range dependencies on graphs. On the other hand, the GrokFormer fits all N eigenvectors capturing the global information. However, fixed-order polynomial filters are local. (2) Flexibility. The graph spectral convolution module in our GrokFormer learns spectrum frequency and order adaptive filter functions, whereas spectral GNNs leverage truncated and linear polynomial bases to approximate filters, limiting their expressiveness and flexibility. (3) Universality. The polynomial spectral GNNs can be used as a filter learning module in the GrokFormer.

Comparison to Graph Transformers. Most GTs can only capture low-frequency information due to the low-pass property of self-attention [39]. Therefore, they do not show competitiveness in node-level tasks when faced with complex node label distributions. Although some improved GTs have been proposed to capture different frequency information, they still have certain weaknesses. For instance, SignGT [39] designed a signed attention mechanism but can only capture low-frequency and high-frequency information. FeTA [14] and PolyFormer [22] aim to capture rich frequency information through learning polynomial spectral filtering, but they share the same drawbacks as polynomial spectral GNNs. Specformer effectively encodes all eigenvalues through self-attention but is restricted to the first-order graph spectrum. Additionally, its self-attention-based filter learning introduces a computational complexity of $O(N^2)$ and numerous free parameters, making it both inefficient and susceptible to overfitting. In contrast, our GrokFormer learns eigenvalue-target functions by Fourier series expansion, which offering higher computational efficiency than self-attention, and flexibly capture K order rich frequency signals, thus performing well on a range of graph tasks. Besides, Specformer and PolyFormer focus only on node representation learning in the spectral domain, while our method captures global graph information from both the spatial and spectral domains, making our approach more general.

TABLE II: Statistics of node classification datasets. A larger \mathcal{H} indicates a stronger (weaker) graph homophily (heterophily).

Datasets	Cora	Citeseer	Pubmed	Photo	Physics	Penn94	Chameleon	Squirrel	Actor	Texas
#Nodes	2,708	3,327	19,717	7,650	34,493	41,554	2,277	5,201	7,600	183
#Edges	5,429	4,732	44,338	238,163	247,962	1,362,229	36,101	217,073	33,544	295
#Features	1,433	3,703	500	745	500	4,814	2,325	2,089	931	1,703
#Classes	7	6	3	8	5	2	5	5	5	5
\mathcal{H}	0.81	0.74	0.80	0.83	0.91	0.47	0.23	0.22	0.22	0.06

TABLE III: Node classification results on five homophilic and five heterophilic datasets: mean accuracy (%) \pm std. The best results are in bold, while the second-best ones are underlined. ‘OOM’ means out of memory

	Homophilic					Heterophilic				
	Cora	Citeseer	Pubmed	Photo	Physics	Penn94	Chameleon	Squirrel	Actor	Texas
Spatial-based GNNs										
GCN	87.14 \pm 1.01	79.86 \pm 0.67	86.74 \pm 0.27	88.26 \pm 0.73	97.74 \pm 0.35	82.47 \pm 0.27	59.61 \pm 2.21	46.78 \pm 0.87	33.23 \pm 1.16	77.38 \pm 3.28
GAT	88.03 \pm 0.79	80.52 \pm 0.71	87.04 \pm 0.24	92.94 \pm 0.44	97.82 \pm 0.28	81.53 \pm 0.55	63.13 \pm 1.93	44.49 \pm 0.88	33.93 \pm 2.47	80.82 \pm 2.13
H2GCN	87.96 \pm 0.37	80.90 \pm 1.21	89.18 \pm 0.28	95.45 \pm 0.67	97.19 \pm 0.13	81.31 \pm 0.60	61.20 \pm 4.28	39.53 \pm 0.88	36.31 \pm 2.58	91.89 \pm 3.93
HopGNN	88.68 \pm 1.06	80.38 \pm 0.68	89.15 \pm 0.35	94.49 \pm 0.33	97.86 \pm 0.16	OOM	65.25 \pm 3.49	57.83 \pm 2.11	39.33 \pm 2.79	89.15 \pm 4.04
Spectral-based GNNs										
ChebyNet	86.67 \pm 0.82	79.11 \pm 0.75	87.95 \pm 0.28	93.77 \pm 0.32	97.25 \pm 0.78	81.55 \pm 0.26	59.28 \pm 1.25	40.55 \pm 0.42	37.61 \pm 0.89	86.22 \pm 2.45
GPR-GNN	88.57 \pm 0.69	80.12 \pm 0.83	88.46 \pm 0.33	93.85 \pm 0.28	97.25 \pm 0.13	81.38 \pm 0.16	67.28 \pm 1.09	50.15 \pm 1.92	39.92 \pm 0.67	92.95 \pm 1.31
BernNet	88.52 \pm 0.95	80.09 \pm 0.79	88.48 \pm 0.41	93.63 \pm 0.35	97.36 \pm 0.30	82.47 \pm 0.21	68.29 \pm 1.58	51.35 \pm 0.73	41.79 \pm 1.01	93.12 \pm 0.65
JacobiConv	88.98 \pm 0.46	80.78 \pm 0.79	89.62 \pm 0.41	95.43 \pm 0.23	97.56 \pm 0.28	83.35 \pm 0.11	74.20 \pm 1.03	57.38 \pm 1.25	41.17 \pm 0.64	93.44 \pm 2.13
HiGCN	89.23 \pm 0.23	81.12 \pm 0.28	89.95 \pm 0.13	95.33 \pm 0.37	97.65 \pm 0.35	OOM	68.47 \pm 0.45	51.86 \pm 0.42	41.81 \pm 0.52	92.15 \pm 0.73
Graph Transformers										
Transformer	76.29 \pm 1.95	76.68 \pm 1.21	86.66 \pm 0.50	89.58 \pm 1.05	OOM	OOM	45.21 \pm 2.01	33.17 \pm 1.32	39.95 \pm 0.64	88.75 \pm 6.30
NodeFormer	87.32 \pm 0.92	79.56 \pm 1.10	89.24 \pm 0.23	95.27 \pm 0.22	96.45 \pm 0.28	69.66 \pm 0.83	56.34 \pm 1.11	43.42 \pm 1.62	34.62 \pm 1.82	84.63 \pm 3.47
SGFormer	87.87 \pm 2.67	79.62 \pm 1.63	89.07 \pm 0.14	94.34 \pm 0.23	97.96 \pm 0.81	76.65 \pm 0.49	61.44 \pm 1.37	45.82 \pm 2.17	41.69 \pm 0.63	92.46 \pm 1.48
NAGphormer	88.15 \pm 1.35	80.12 \pm 1.24	89.70 \pm 0.19	95.49 \pm 0.11	97.85 \pm 0.26	73.98 \pm 0.53	54.92 \pm 1.11	48.55 \pm 2.56	40.08 \pm 1.50	91.80 \pm 1.85
Specformer	88.57 \pm 1.01	81.49 \pm 0.94	90.61 \pm 0.23	95.48 \pm 0.32	97.75 \pm 0.53	84.32\pm0.32	74.72 \pm 1.29	64.64 \pm 0.81	41.93 \pm 1.04	88.23 \pm 0.38
PolyFormer(Cheb)	87.67 \pm 1.28	81.80 \pm 0.76	90.68 \pm 0.31	94.08 \pm 1.37	98.08 \pm 0.27	79.27 \pm 0.26	60.17 \pm 1.39	44.98 \pm 3.03	41.51 \pm 0.71	89.02 \pm 5.44
GrokFormer	89.57\pm1.43	81.92\pm1.25	91.39\pm0.51	95.52\pm0.52	98.31\pm0.18	83.59 \pm 0.26	75.58\pm1.73	65.12\pm1.59	42.98\pm1.48	94.59\pm2.08

V. EXPERIMENTS

In this section, we conduct comprehensive experiments on a wide range of real-world graph datasets in both node classification and graph classification tasks to verify the effectiveness of our GrokFormer. Then, we evaluate the ability of GrokFilter on synthetic and real-world datasets. Finally, we conduct the ablation study, parameter analysis, and complexity comparison experiments.

For the implementation, we utilize NetworkX, Pytorch, and Pytorch Geometric for model construction. All experiments are conducted on NVIDIA GeForce RTX 3090 GPUs with 24 GB memory, TITAN Xp GPU machines equipped with 12 GB memory. Following the previous work [25], [26], classification accuracy is used as a metric to evaluate the performance of all models in node and graph classification tasks, which denotes the percentage of nodes/graphs whose labels are correctly classified.

A. Node Classification

Dataset Description. We conduct node classification experiments on 10 widely used datasets, including five homophilic and five heterophilic datasets. For homophilic datasets, we adopt three citation graphs Cora, Citeseer, Pubmed, an Amazon co-purchase graph Photo [17], and a co-authorship network Physics [48]. For heterophilic graphs, we adopt the Wikipedia graphs Chameleon and Squirrel, the Actor co-occurrence graph [49], webpage graphs Texas from WebKB¹,

and Penn94, a large-scale friendship network from the Facebook 100 networks [50]. Following the previous works [13], [17], the node set was split into train/validation/test set with ratio 60%/20%/20%. We summarize the statistics of these datasets in Table II.

Baselines and Settings. We compare GrokFormer with fifteen competitive baselines, including (i) four spatial-based GNNs: GCN [25], GAT [26], H2GCN [29] and HopGNN [30], (ii) five spectral-based GNNs: ChebyNet [20], GPR-GNN [18], BernNet [17], JacobiConv [21] and HiGCN [33], and (iii) six GTs: vanilla Transformer [1], NodeFormer [36], SGFormer [12], NAGphormer [45], Specformer [13] and PolyFormer(Cheb) [22]. For fairness, we generate 10 random splits and evaluate all models on the same splits, and report the average metric for each model. For polynomial GNNs, we set the order of polynomials $K = 10$, consistent with their original setting. In addition to the above settings, for the baseline models, we adopt the best hyperparameters provided by the authors if available, and we meticulously fine-tune the parameters to achieve good performance otherwise. If the baseline methods are consistent with our dataset partition and the experimental results we run are close to their paper reported, we directly use the results provided by the authors. We train the proposed GrokFormer model with the learning rate $lr \in \{0.005, 0.01\}$, the weight decay $wd \in \{0.001, 0.005, 0.0001, 0.0005, 0.00005\}$, dropout $\in \{0.0, 0.1, \dots, 0.8\}$ with step 0.1, and $M \in \{16, 32\}$. We set GrokFormer to adaptively cover the spectrum from the 1st up to 6-th order, i.e., $K \in \{1, 2, \dots, 6\}$.

¹<http://www.cs.cmu.edu/afs/cs.cmu.edu/project/theo-11/www/wwkb>

TABLE IV: Statistics of graph classification datasets

Datasets	PROTEINS	MUTAG	PTC-MR	IMDB-B	IMDB-M
#Graphs	1113	188	344	1000	1500
#Classes	2	2	2	2	3
#Nodes (Max)	620	28	109	136	89
#Nodes (Avg.)	39.06	17.93	14.29	19.77	13.00
#Edges (Avg.)	72.82	19.79	14.69	13.06	65.93

Due to the increased number of nodes and edges, we set $K = 10$ for the large-scale dataset Penn94. We leverage Adam as the model optimizer and establish the maximum number of epochs at 2,000 for all datasets. In the large-scale datasets Physics and Penn94, we implement truncated spectral decomposition for both GrokFormer and Specformer to enhance scalability, selecting the 3,000 eigenvectors associated with the smallest (low-frequency) and largest (high-frequency) eigenvalues.

Results. From Table III, we can observe that (1) GrokFormer achieves excellent performance, exceeding state-of-the-art baselines on across both homophilic and heterophilic datasets, which validates our model’s ability to learn adaptive high-quality node representations on datasets with different level of homophily/heterophily. (2) Except for the Transformer, which does not consider graph topology information, almost all baseline methods perform well on homophilic datasets. This is most likely because graph models can easily capture the similarity information between neighbors, and low-pass filtering is easier to fit in homophilic networks. (3) In heterophilic networks, all baseline methods except Specformer fail to perform satisfactorily due to their limited learning ability. Specformer and our GrokFormer can learn and fit complex filters to capture rich frequency information by considering all eigenvalues, thus enhancing learning and expression capabilities, and performing well in heterophilic networks. (4) Compared to Specformer, our GrokFormer performs better because our model efficiently and flexibly captures more graph information than Specformer from K different graph spectral orders. In addition, Specformer learns node representations solely from the spectral domain, whereas our GrokFormer takes into account both spectral and spatial information simultaneously. (5) GrokFormer can also be used in large-scale graph datasets Physics and Penn94 using efficient self-attention and truncated decomposition to reduce time and space costs.

B. Graph Classification

Dataset. We conduct graph classification experiments on five datasets from diverse domains to evaluate the performance of the proposed GrokFormer. The datasets are divided into two main categories: bioinformatics datasets and social network datasets. The bioinformatics datasets include PROTEINS [51], PTC-MR [52], and MUTAG [53], where the graphs denote chemical compounds. Two social network datasets IMDB-BINARY and IMDB-MULTI [54], where the graph originates from a specific movie genre, nodes represent actors/actresses, and edges connect them if they appear in the same movie. The statistics of these datasets are summarized in Table IV.

TABLE V: Graph classification results. The best results are in bold, while the second-best ones are underlined

	PROTEINS	MUTAG	PTC-MR	IMDB-B	IMDB-M
Kernel methods					
GK	71.4 \pm 0.3	81.7 \pm 2.1	55.3 \pm 1.4	65.9 \pm 1.0	43.9 \pm 0.4
WL kernel	75.0 \pm 3.1	90.4 \pm 5.7	59.9 \pm 4.3	73.8 \pm 3.9	50.9 \pm 3.8
DGK	71.7 \pm 0.5	82.7 \pm 1.4	57.3 \pm 1.1	67.0 \pm 0.6	44.6 \pm 0.5
GNN methods					
DGCNN	75.5 \pm 0.9	85.8 \pm 1.8	58.6 \pm 2.5	70.0 \pm 10.9	47.8 \pm 10.9
GCN	75.2 \pm 2.8	85.1 \pm 3.8	63.1 \pm 4.3	73.8 \pm 3.4	55.2 \pm 0.3
GIN	76.2 \pm 2.8	89.4 \pm 5.6	64.6 \pm 7.0	75.1 \pm 5.1	52.3 \pm 2.8
GDN	81.3 \pm 3.1	97.4 \pm 2.7	75.6 \pm 7.6	79.3 \pm 3.3	55.2 \pm 4.3
HiGCN	77.0 \pm 4.2	91.3 \pm 6.4	66.2 \pm 6.9	76.2 \pm 5.1	52.7 \pm 3.5
Graph Transformers					
Transformer	66.3 \pm 8.4	81.9 \pm 9.7	57.3 \pm 7.0	71.1 \pm 3.8	45.8 \pm 3.8
Graphormer	68.5 \pm 2.3	82.5 \pm 3.8	59.2 \pm 4.6	73.5 \pm 3.8	48.9 \pm 2.3
SGFormer	74.6 \pm 3.0	88.6 \pm 6.3	65.2 \pm 4.2	74.7 \pm 4.1	56.4 \pm 3.4
NAGphormer	72.5 \pm 2.3	89.9 \pm 10.4	66.5 \pm 5.6	75.1 \pm 4.3	51.7 \pm 3.5
Specformer	70.9 \pm 6.0	96.3 \pm 5.3	82.9 \pm 4.9	86.6 \pm 2.7	58.5 \pm 3.9
GrokFormer	78.2 \pm 2.4	99.5 \pm 1.6	94.8 \pm 2.5	88.5 \pm 2.3	62.2 \pm 3.0

Baselines and Settings. We compare our GrokFormer with three prevalent graph classification models, including three kernel-based methods: GK [55], WL kernel [56] and DGK [54], five popular GNN-based models: DGCNN [57], GCN, GIN [58], GDN [59], and HiGCN, as well as five graph transformer models: Transformer, Graphormer [9], SGFormer, NAGphormer, Specformer. We follow the same evaluation protocol of InfoGraph [60] to conduct a 10-fold cross-validation scheme for a fair comparison and report the maximum average validation accuracy across folds. We set the hyper-parameters of the baseline methods suggested by their authors. For the proposed GrokFormer, the hyperparameter space used for experiments is enumerated follows: learning rate $lr \in \{0.001, 0.005, 0.0005, 0.0001\}$, the weight decay $wd \in \{0.0, 0.0005, 0.00005\}$, the hidden dimension $d \in \{32, 64\}$, the batch size is searched in $\{32, 64, 128\}$. We implement readout operations by conducting max pooling to obtain a global embedding for each graph.

Results. The performance of graph classification is presented in Table V. We find that the proposed models outperform state-of-the-art baselines on 4 out of 5 datasets and achieve 11.9% relative improvement on the PTC-MR, which validates the superiority of our GrokFormer. In addition, compared to the kernel-based model, our approaches achieve a greater improvement, with a maximum improvement of 34.9% on the PTC-MR dataset. In contrast, GNN methods and graph Transformers usually perform better than traditional kernel methods. GrokFormer shows consistent superiority over the strongest baseline, Specformer, achieving an average improvement of 5.6% across all datasets, although it records a slightly lower score in the PROTEINS dataset. GrokFormer exhibits remarkable capabilities in graph representation learning by effectively capturing complex and desired frequency signals from the first- to higher-order graph spectrum, surpassing the performance of these baselines.

C. Effectiveness of Graph Fourier KAN Filters

1) *Fitting Signals on Synthetic Datasets.* : In this subsection, we assess the effectiveness of the adaptive filter learning

TABLE VI: Node regression results, mean of the sum of squared error and R^2 score, on synthetic data

Models	Low-pass	High-pass	Band-pass	Band-rejection	Comb
	$\exp(-10\lambda^2)$	$1-\exp(-10\lambda^2)$	$\exp(-10(\lambda-1)^2)$	$1-\exp(-10(\lambda-1)^2)$	$ \sin(\pi\lambda) $
GCN	3.5149(.9872)	68.6770(.2400)	26.2434(.1074)	21.0127(.9440)	49.8023(.3093)
GAT	2.6883(.9898)	21.5288(.7447)	13.8871(.4987)	12.9724(.9643)	22.0646(.6998)
ChebyNet	0.8284(.9973)	0.7796(.9902)	2.3071(.9100)	2.5455(.9934)	4.0355(.9455)
GPR-GNN	0.4378(.9983)	0.1046(.9985)	2.1593(.8952)	4.2977(.9894)	4.9416(.9283)
BernNet	0.0319(.9999)	0.0146(.9998)	0.0388(.9984)	0.9419(.9973)	1.1073(.9853)
PolyAttn(Cheb)	0.0104(.9999)	0.0125(.9998)	0.0394(.9981)	0.7337(.9978)	3.9672(.9443)
Specformer	0.0020(.9999)	0.0029(.9999)	0.0010(.9999)	0.0038(.9999)	0.0063(.9998)
GrokFilter	0.0016(.9999)	0.0017(.9999)	0.0004(.9999)	0.0024(.9999)	0.0021(.9999)

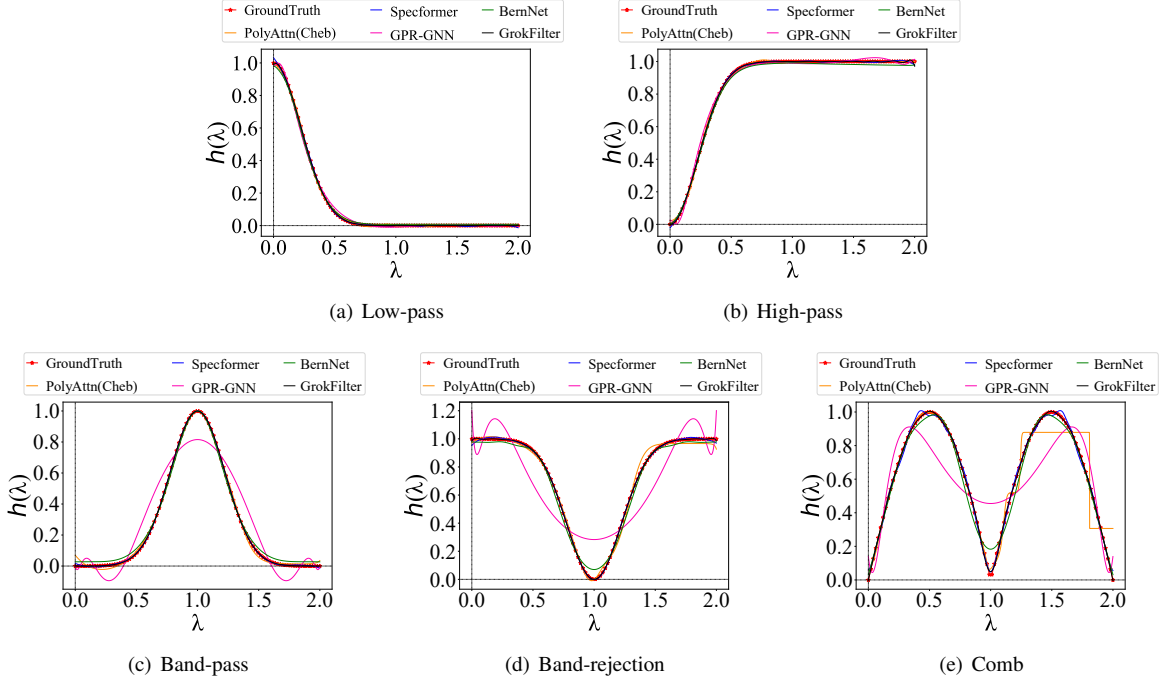


Fig. 3: Illustrations of five filters and their approximations learned by our GrokFilter and other spectral GNNs.

module of GrokFormer, *i.e.*, namely Graph Fourier KAN Filter (GrokFilter), using synthetic datasets. This evaluation highlights the improved abilities of GrokFilter in learning filter patterns, without requiring any prior knowledge of predefined filters.

Synthetic Datasets. Following prior works [13], [17], we conduct experiment using 50 real images with a resolution of 100×100 from the Image Processing in Matlab library². Each image can be represented as a 2d regular grid graph with 4-neighborhood connectivity. The pixel values serve as node signals ranging from 0 to 1. The m -th image has an adjacency matrix $\mathbf{A}_m \in \mathbb{R}^{10000 \times 10000}$ and a node signal $x_m \in \mathbb{R}^{10000}$. For each image, we apply different predefined filters to the spectral domain of its signal, with each filter detailed in Table VI. Models are expected to learn these predefined filtering patterns.

Setup. We compare GrokFilter with seven baseline methods, including GCN, GAT, ChebyNet, GPR-GNN, BernNet, PolyAttn(Cheb) [22] and Specformer. To ensure a fair compar-

ison, we adjust the number of hidden units to maintain nearly 2K parameters for all models and set the polynomial order K to 10 for ChebyNet, GPR-GNN, and BernNet. In addition, we uniformly set the learning rate to 0.01, and the training epochs to 2,000 with the patience of early stop 100. We assess each method based on two criteria: the sum of squared errors, where lower values are desirable, and the R^2 score, which should be maximized.

Results. Table VI reports the average of the sum of squared error and the R^2 scores. We can observe that (1) GrokFilter consistently achieved superior performance compared to these baseline models in two metrics. For complex graph filters, such as Comb and Band, our method performs well, proving the effectiveness of GrokFilter in learning complex graph filters. (2) GCN and GAT can only learn low-pass filter well, which is not enough in heterophilic graph learning. (3) Polynomial-based spectral GNNs, ChebyNet, GPR-GNN, and BernNet perform better than GCN by approximating graph filtering using polynomials. However, the expressiveness of their linear polynomials is still limited in learning complex filters. (4)

²<https://ww2.mathworks.cn/products/image.html>

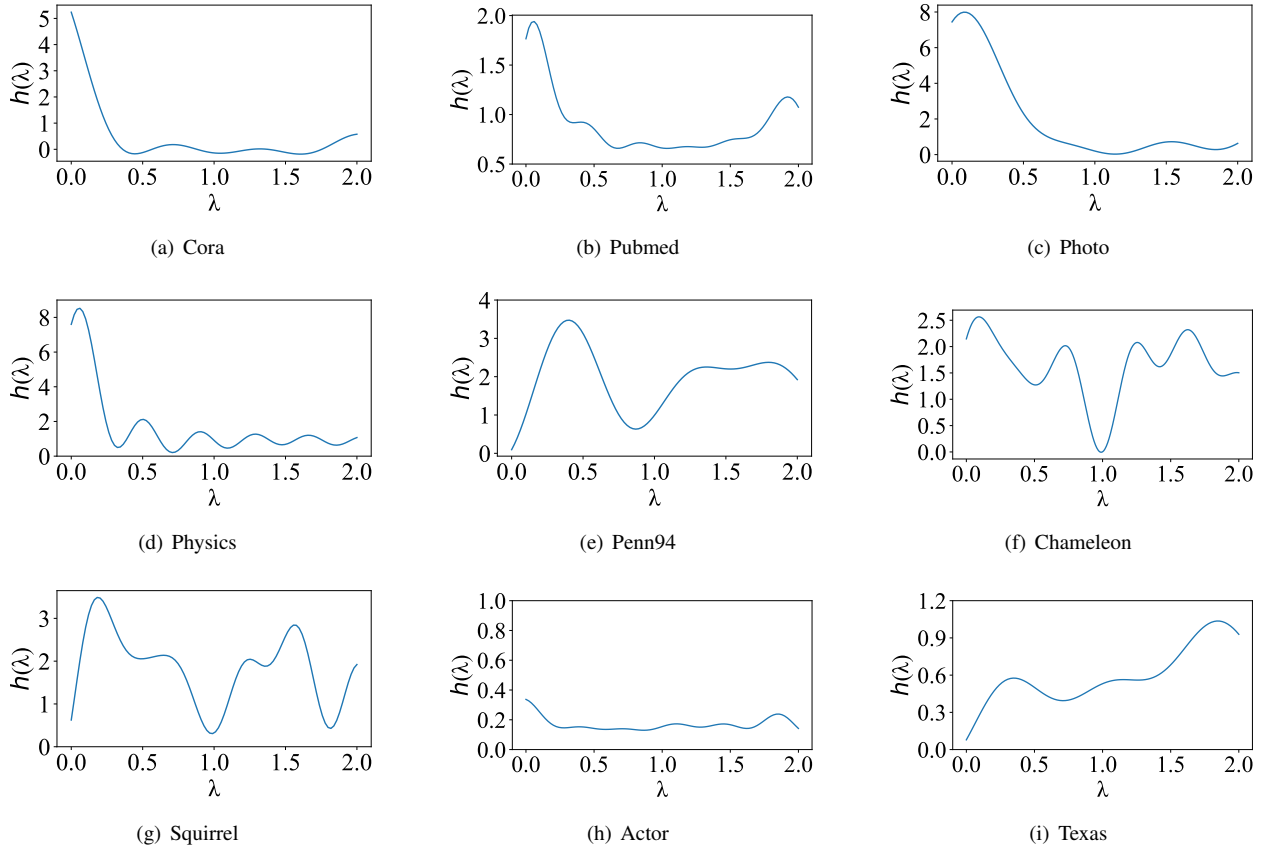


Fig. 4: Filters learned from nine real-world datasets by our GrokFilter.

PolyAttn(Cheb) executes non-linear on polynomials obtains better results than linear polynomials, but it fails in capturing the complex filter patterns in Comb. (5) Specformer performs self-attention on eigenvalues possessing a stronger expression ability than polynomial filters, but it is still weaker than our GrokFilter.

Additionally, we present a visualization of the graph filter learning obtained from GPR-GNN, BernNet, Specformer, PolyAttn(Cheb) and GrokFilter in Fig. 3, providing further support for our method. We can see that low-pass and high-pass filters are easy to fit for them, but polynomial GNNs and PolyAttn(Cheb) are difficult to fit complex filters: Band pass, Band-rejection pass, and Comb, which will hurt their performance. Although Specformer has been well fitted, our GrokFilter is superior in comparison, once again reflecting the excellent capability of GrokFilter to learn graph filters.

2) *Performance on Real-world Datasets.*: We conduct this experiment on nine real-world node classification datasets to evaluate the efficacy of our GrokFilter.

Setup. The experimental setting is the same as the node classification task, as stated in settings of Section V-A.

Results. As shown in Fig. 4, we plot the filtering curve $h(\lambda)$ learned by the GrokFilter module on nine different datasets. From Fig. 4, we can observe that (1) on homophilic graphs, GrokFilter learns low-pass filters with different amplitude and

TABLE VII: Ablation studies on node- and graph-level tasks

Tasks	Datasets	*-w/o-GrokFilter	GrokFilter	GrokFormer
Node	Cora	77.42±1.77	88.98±1.25	89.57±1.43
	Citeseer	77.12±1.19	81.57±1.80	81.92±1.25
	Pubmed	86.58±0.79	90.76±0.46	91.39±0.51
	Photo	89.58±1.05	95.10±0.78	95.52±0.52
	Physics	97.06±0.42	98.27±0.21	98.31±0.18
	Penn94	75.19±0.36	80.57±0.16	83.59±0.26
	Chameleon	45.03±1.80	74.97±1.67	75.58±1.73
	Squirrel	32.25±1.83	64.57±1.59	65.12±1.59
	Actor	40.95±2.05	42.15±1.29	42.98±1.48
Graph	Texas	90.33±2.36	93.62±3.04	94.59±2.08
	PROTEINS	71.4±3.7	76.1±3.5	78.2±2.4
	MUTAG	82.1±5.9	98.9±2.2	99.5±1.6
	PTC-MR	61.6±6.2	92.4±6.7	94.8±2.5
	IMDB-B	74.9±3.8	87.3±2.5	88.5±2.3
	IMDB-M	51.7±3.1	61.9±4.6	62.2±3.0

frequency responses for them, which is consistent with the homophily property, i.e., the low-frequency information is important in the homophilic scenario. (2) On Chameleon and Squirrel, GrokFilter learns comb-alike filters with complex frequency components. Meanwhile, we find that our GrokFilter outperforms baselines on these two datasets in Table III, this indicates that our method learns the complex frequency responses that are difficult for other methods to capture but are essential for Chameleon and Squirrel. (3) GrokFilter learns

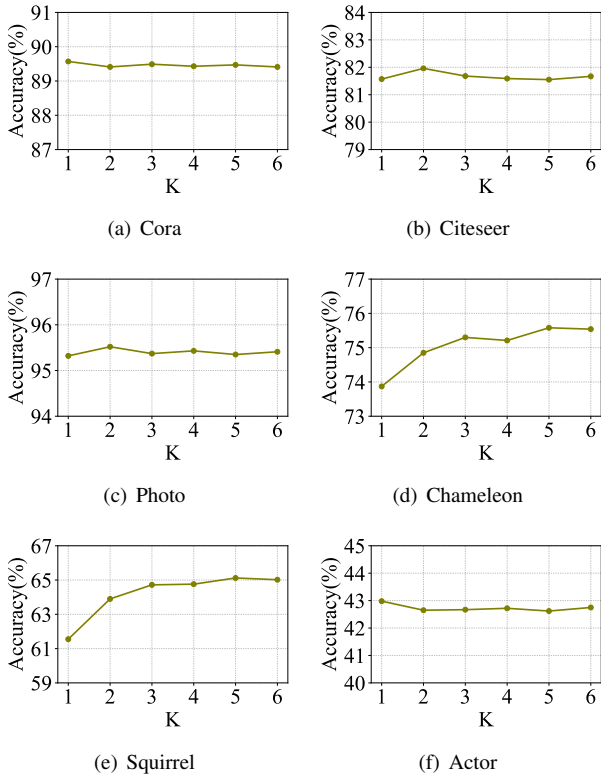


Fig. 5: Analysis results of the order K on three homophilic and three heterophilic datasets.

an all-pass filter on the Actor dataset protecting its raw features, which is consistent with the fact that its raw features are associated with labels [17]. (4) In heterophilic graph Texas, GrokFilter learns a high-pass filter, which matches the strong heterophily, i.e., the high-frequency information that captures the difference between nodes is important. Compared to the filter learned on Texas, the filter learned on Penn94 retain relatively more low-frequency components due to its higher homophily than Texas. In summary, our GrokFilter can adaptively learn various required filter functions for networks with different properties under the Transformer architecture to help capture the desired frequency response beyond the low-frequency retained by the self-attention mechanism.

D. Ablation Study

This section conducts an ablation study on ten node classification and five graph classification datasets. As ablation study models, we present two distinct models: i) the first ablation model, designated as **-w/o-GrokFilter*, incorporates only the efficient self-attention module of GrokFormer, without the spectral graph convolution module; ii) the second model is the spectral graph convolution module GrokFilter, excluding the self-attention. The mean classification results of the ablation study are reported in Table VII. The following observations can be derived:

(1) GrokFormer consistently outperforms its variants across all datasets on different graph tasks, demonstrating that the

designed GrokFilter in the GrokFormer contributes to capturing various frequency information beyond low frequency, and cooperates with self-attention to learn the precise and informative node representations and improving performance. (2) The performance of GrokFilter is generally better than **-w/o-GrokFilter* on all datasets, which shows that the frequency adaptive for node/graph representation learning plays an important role. (3) On the node-level task, **-w/o-GrokFilter* is difficult to perform well on homophilic datasets due to the loss of important graph structure information, but it performs well on heterophilic networks (Actor and Texas) with a high correlation between feature information and node labels. This finding shows that the self-attention in spatial domain and GrokFilter in spectral domain are both useful. (4) Comparing the node classification results in Tables VII and III, as well as the graph classification results in Tables VII and V, GrokFilter still maintains competitive performance against the baselines offering powerful expression capabilities, and demonstrating that GrokFormer is effective and competitive across a range of graph tasks.

E. Hyperparameter Analysis

To study the impact of the graph spectral order, we conduct analytical experiments regarding the order K on six node classification datasets with different homophily. We vary the order K from one to six to observe the change of the node classification accuracy. As shown in Fig. 5, the optimal value of K for GrokFormer varies across different datasets because the graph properties of each dataset are different, which shows that it is necessary to learn graph filters from K -order graph information. We can find that GrokFormer achieves the best accuracy on Squirrel and Chameleon when K is greater than three, but on other datasets, optimal performance usually occurs when K is less than three. Meanwhile, combining the learned filtering curves in Fig. 4, we draw the following conclusions: Squirrel and Chameleon usually require more complex frequency responses than other datasets. It will be insufficient to learn the filter function only from the first-order graph spectrum. The higher-order filter learning can help Squirrel and Chameleon to enrich the frequency response and adaptively capture the desired frequency signals. Therefore, Squirrel and Chameleon achieve the best results at larger values of K . For other datasets, they expect the low-pass filter and the all-pass filter. These simple filters tend to be easy to learn, so they extract the desired frequency response when K is small.

F. Complexity Comparison

This subsection evaluates GrokFormer in comparison to other attention-based models on the Photo dataset concerning classification accuracy, training time, and the total number of parameters. Note that the model training time does not include preprocessing. To ensure all models have similar numbers of parameters on the Photo dataset, we set the hidden size $d = 32$. For PolyFormer(Cheb), we set the order of polynomials

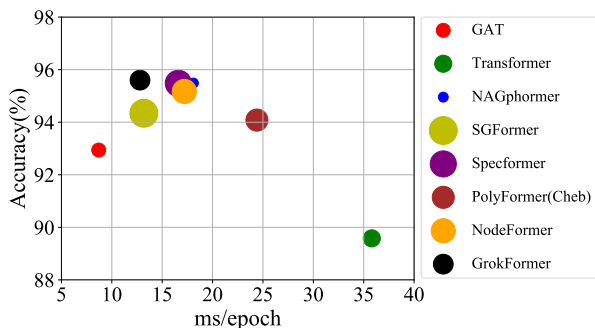


Fig. 6: Accuracy and training time on Photo.

$K = 10$ as suggested. For NAGphormer, we set the number of hops $h = 7$ to be consistent with its original setting.

As shown in Fig. 6, the x-axis represents training time, the y-axis represents classification accuracy, and the area of the circle indicates the total relative numbers of parameters. From Fig. 6, we can observe that GrokFormer achieves the best performance with low training time and few parameters. SGFormer designs simple global attention and achieves $O(N)$ time complexity in self-attention, so it is much more efficient than others. NodeFormer adds a new loss function compared to the other methods, thus increasing part of the training time. NAGphormer needs to obtain the h -hop features by calculating $\mathbf{A}\mathbf{X}$ h times. To reduce computational complexity, NAGphormer precomputes the h -hop features. However, it inevitably requires dimensionality reduction on features with h times the original dimension size, resulting in this part of the complexity being h times that of other methods. Specformer and our model utilize a 2-layer MLP (embedding layer) on the feature matrix \mathbf{X} to reduce the feature dimension F to number of classes C ($C \ll F$) before information passing, which is identical to that of previous models BernNet and GPR-GNN. This propagation process reduces their time complexity, thus faster than PolyFormer(Cheb). Compared to the Specformer, our GrokFormer trains faster utilizing efficient self-attention mechanism and filter learning method.

VI. CONCLUSION AND FUTURE WORK

This paper presents GrokFormer, a novel GT model that integrates an adaptive spectral filter learning module and self-attention to effectively capture a broad spectrum of frequency information from K order graph spectrum. By learning spectral filters from the multi-order graph spectrum, GrokFormer succeeds in preserving long-range dependencies while effectively capturing intricate node relationships characterized by various frequency information. In this way, GrokFormer significantly improves classification accuracy by enriching the learned node representations in diverse real-world scenarios, including those exhibiting high heterophily. Our comprehensive experiments demonstrated that GrokFormer consistently outperforms a range of baseline methods across node classification and graph classification tasks.

The GrokFormer presents a promising approach to semi-supervised learning, leveraging guided learning with a limited number of labeled samples. However, when labeled samples are scarce, GrokFormer may struggle to extract the desired frequency information. A key avenue for future research involves enhancing the model’s capabilities in unsupervised learning, transfer learning, and contrastive learning to mitigate the challenges associated with a lack of labeled data.

REFERENCES

- [1] A. Vaswani, N. Shazeer, N. Parmar, J. Uszkoreit, L. Jones, A. N. Gomez, L. Kaiser, and I. Polosukhin, “Attention is all you need,” *Advances in Neural Information Processing Systems*, vol. 30, 2017.
- [2] A. Dosovitskiy, L. Beyer, A. Kolesnikov, D. Weissenborn, X. Zhai, T. Unterthiner, M. Dehghani, M. Minderer, G. Heigold, S. Gelly *et al.*, “An image is worth 16x16 words: Transformers for image recognition at scale,” in *International Conference on Learning Representations*, 2020.
- [3] J. Zhang, H. Zhang, C. Xia, and L. Sun, “Graph-bert: Only attention is needed for learning graph representations,” *arXiv preprint arXiv:2001.05140*, 2020.
- [4] V. P. Dwivedi and X. Bresson, “A generalization of transformer networks to graphs,” *arXiv preprint arXiv:2012.09699*, 2020.
- [5] D. Kreuzer, D. Beaini, W. Hamilton, V. Létourneau, and P. Tossou, “Rethinking graph transformers with spectral attention,” *Advances in Neural Information Processing Systems*, vol. 34, pp. 21 618–21 629, 2021.
- [6] J. Kim, D. Nguyen, S. Min, S. Cho, M. Lee, H. Lee, and S. Hong, “Pure transformers are powerful graph learners,” *Advances in Neural Information Processing Systems*, vol. 35, pp. 14 582–14 595, 2022.
- [7] Z. Wu, P. Jain, M. Wright, A. Mirhoseini, J. E. Gonzalez, and I. Stoica, “Representing long-range context for graph neural networks with global attention,” *Advances in Neural Information Processing Systems*, vol. 34, pp. 13 266–13 279, 2021.
- [8] L. Maziarka, T. Danel, S. Mucha, K. Rataj, J. Tabor, and S. Jastrzebski, “Molecule attention transformer,” *arXiv preprint arXiv:2002.08264*, 2020.
- [9] C. Ying, T. Cai, S. Luo, S. Zheng, G. Ke, D. He, Y. Shen, and T.-Y. Liu, “Do transformers really perform badly for graph representation?” *Advances in neural information processing systems*, vol. 34, pp. 28 877–28 888, 2021.
- [10] D. Chen, L. O’Bray, and K. Borgwardt, “Structure-aware transformer for graph representation learning,” in *International Conference on Machine Learning*, 2022, pp. 3469–3489.
- [11] K. Choromanski, H. Lin, H. Chen, T. Zhang, A. Sehanobish, V. Likhosherstov, J. Parker-Holder, T. Sarlos, A. Weller, and T. Weingarten, “From block-toeplitz matrices to differential equations on graphs: towards a general theory for scalable masked transformers,” in *International Conference on Machine Learning*, 2022, pp. 3962–3983.
- [12] Q. Wu, W. Zhao, C. Yang, H. Zhang, F. Nie, H. Jiang, Y. Bian, and J. Yan, “Simplifying and empowering transformers for large-graph representations,” *Advances in Neural Information Processing Systems*, vol. 36, 2024.
- [13] D. Bo, C. Shi, L. Wang, and R. Liao, “Specformer: Spectral graph neural networks meet transformers,” in *The Eleventh International Conference on Learning Representations*, 2023.
- [14] A. Bastos, A. Nadgeri, K. Singh, H. Kanezashi, T. Suzumura, and I. O. Mulang, “How expressive are transformers in spectral domain for graphs?” *Transactions on Machine Learning Research*, 2022.
- [15] P. Wang, W. Zheng, T. Chen, and Z. Wang, “Anti-oversmoothing in deep vision transformers via the fourier domain analysis: From theory to practice,” in *International Conference on Learning Representations*, 2022.
- [16] H. Shi, J. GAO, H. Xu, X. Liang, Z. Li, L. Kong, S. M. Lee, and J. Kwok, “Revisiting over-smoothing in bert from the perspective of graph,” in *International Conference on Learning Representations*, 2022.
- [17] M. He, Z. Wei, H. Xu *et al.*, “Bernnet: Learning arbitrary graph spectral filters via bernstein approximation,” *Advances in Neural Information Processing Systems*, vol. 34, pp. 14 239–14 251, 2021.
- [18] E. Chien, J. Peng, P. Li, and O. Milenkovic, “Adaptive universal generalized pagerank graph neural network,” in *9th International Conference on Learning Representations, ICLR 2021*, 2021.

- [19] H. Qiao and G. Pang, "Truncated affinity maximization: One-class homophily modeling for graph anomaly detection," *Advances in Neural Information Processing Systems*, vol. 36, 2024.
- [20] M. Defferrard, X. Bresson, and P. Vandergheynst, "Convolutional neural networks on graphs with fast localized spectral filtering," *Advances in neural information processing systems*, vol. 29, 2016.
- [21] X. Wang and M. Zhang, "How powerful are spectral graph neural networks," in *International conference on machine learning*, 2022, pp. 23 341–23 362.
- [22] J. Ma, M. He, and Z. Wei, "Polyformer: Scalable node-wise filters via polynomial graph transformer," in *Proceedings of the 30th ACM SIGKDD Conference on Knowledge Discovery and Data Mining*, 2024, pp. 2118–2129.
- [23] H. Qiao, H. Tong, B. An, I. King, C. Aggarwal, and G. Pang, "Deep graph anomaly detection: A survey and new perspectives," *arXiv preprint arXiv:2409.09957*, 2024.
- [24] B. Xu, H. Shen, Q. Cao, K. Cen, and X. Cheng, "Graph convolutional networks using heat kernel for semi-supervised learning," in *Proceedings of the 28th International Joint Conference on Artificial Intelligence*, 2019, pp. 1928–1934.
- [25] T. N. Kipf and M. Welling, "Semi-supervised classification with graph convolutional networks," in *International Conference on Learning Representations*, 2017.
- [26] P. Veličković, G. Cucurull, A. Casanova, A. Romero, P. Liò, and Y. Bengio, "Graph attention networks," in *International Conference on Learning Representations*, 2018.
- [27] K. Oono and T. Suzuki, "Graph neural networks exponentially lose expressive power for node classification," in *International Conference on Learning Representations*, 2020.
- [28] J. Toppling, F. Di Giovanni, B. P. Chamberlain, X. Dong, and M. M. Bronstein, "Understanding over-squashing and bottlenecks on graphs via curvature," in *International Conference on Learning Representations*, 2022.
- [29] J. Zhu, Y. Yan, L. Zhao, M. Heimann, L. Akoglu, and D. Koutra, "Beyond homophily in graph neural networks: Current limitations and effective designs," *Advances in neural information processing systems*, vol. 33, pp. 7793–7804, 2020.
- [30] J. Chen, Z. Li, Y. Zhu, J. Zhang, and J. Pu, "From node interaction to hop interaction: New effective and scalable graph learning paradigm," in *Proceedings of the IEEE/CVF Conference on Computer Vision and Pattern Recognition*, 2023, pp. 7876–7885.
- [31] Y. Dong, K. Ding, B. Jalaian, S. Ji, and J. Li, "Adagmn: Graph neural networks with adaptive frequency response filter," in *Proceedings of the 30th ACM international conference on information & knowledge management*, 2021, pp. 392–401.
- [32] J. Gasteiger, A. Bojchevski, and S. Günnemann, "Predict then propagate: Graph neural networks meet personalized pagerank," in *International Conference on Learning Representations*, 2018.
- [33] Y. Huang, Y. Zeng, Q. Wu, and L. Lü, "Higher-order graph convolutional network with flower-petals laplacians on simplicial complexes," in *Proceedings of the AAAI Conference on Artificial Intelligence*, vol. 38, no. 11, 2024, pp. 12 653–12 661.
- [34] U. Alon and E. Yahav, "On the bottleneck of graph neural networks and its practical implications," in *International Conference on Learning Representations*, 2020.
- [35] L. Rampásek, M. Galkin, V. P. Dwivedi, A. T. Luu, G. Wolf, and D. Beaini, "Recipe for a general, powerful, scalable graph transformer," *Advances in Neural Information Processing Systems*, vol. 35, pp. 14 501–14 515, 2022.
- [36] Q. Wu, W. Zhao, Z. Li, D. P. Wipf, and J. Yan, "Nodeformer: A scalable graph structure learning transformer for node classification," *Advances in Neural Information Processing Systems*, vol. 35, pp. 27 387–27 401, 2022.
- [37] M. S. Hussain, M. J. Zaki, and D. Subramanian, "Global self-attention as a replacement for graph convolution," in *Proceedings of the 28th ACM SIGKDD Conference on Knowledge Discovery and Data Mining*, 2022, pp. 655–665.
- [38] D. Bo, X. Wang, C. Shi, and H. Shen, "Beyond low-frequency information in graph convolutional networks," in *Proceedings of the AAAI conference on artificial intelligence*, vol. 35, no. 5, 2021, pp. 3950–3957.
- [39] J. Chen, G. Li, J. E. Hopcroft, and K. He, "Signgt: Signed attention-based graph transformer for graph representation learning," *arXiv preprint arXiv:2310.11025*, 2023.
- [40] D. I. Shuman, S. K. Narang, P. Frossard, A. Ortega, and P. Vandergheynst, "The emerging field of signal processing on graphs: Extending high-dimensional data analysis to networks and other irregular domains," *IEEE signal processing magazine*, vol. 30, no. 3, pp. 83–98, 2013.
- [41] Z. Shen, M. Zhang, H. Zhao, S. Yi, and H. Li, "Efficient attention: Attention with linear complexities," in *Proceedings of the IEEE/CVF winter conference on applications of computer vision*, 2021, pp. 3531–3539.
- [42] G. Cybenko, "Approximation by superpositions of a sigmoidal function," *Mathematics of control, signals and systems*, vol. 2, no. 4, pp. 303–314, 1989.
- [43] A. N. Kolmogorov, "On the representation of continuous functions of many variables by superposition of continuous functions of one variable and addition," in *Doklady Akademii Nauk*, vol. 114, no. 5. Russian Academy of Sciences, 1957, pp. 953–956.
- [44] E. O. Brigham and R. Morrow, "The fast fourier transform," *IEEE spectrum*, vol. 4, no. 12, pp. 63–70, 1967.
- [45] J. Chen, K. Gao, G. Li, and K. He, "Nagphormer: A tokenized graph transformer for node classification in large graphs," in *The Eleventh International Conference on Learning Representations*, 2023.
- [46] D. Bo, Y. Fang, Y. Liu, and C. Shi, "Graph contrastive learning with stable and scalable spectral encoding," *Advances in Neural Information Processing Systems*, vol. 36, 2024.
- [47] Y. Cai, G. Fang, and P. Li, "A note on sparse generalized eigenvalue problem," *Advances in Neural Information Processing Systems*, vol. 34, pp. 23 036–23 048, 2021.
- [48] O. Shchur, M. Mumme, A. Bojchevski, and S. Günnemann, "Pitfalls of graph neural network evaluation," *arXiv preprint arXiv:1811.05868*, 2018.
- [49] H. Pei, B. Wei, K. C.-C. Chang, Y. Lei, and B. Yang, "Geom-gcn: Geometric graph convolutional networks," in *8th International Conference on Learning Representations*, 2020.
- [50] D. Lim, F. Hohne, X. Li, S. L. Huang, V. Gupta, O. Bhalerao, and S. N. Lim, "Large scale learning on non-homophilous graphs: New benchmarks and strong simple methods," *Advances in Neural Information Processing Systems*, vol. 34, pp. 20 887–20 902, 2021.
- [51] K. M. Borgwardt, C. S. Ong, S. Schönauer, S. Vishwanathan, A. J. Smola, and H.-P. Kriegel, "Protein function prediction via graph kernels," *Bioinformatics*, vol. 21, no. suppl_1, pp. i47–i56, 2005.
- [52] H. Toivonen, A. Srinivasan, R. D. King, S. Kramer, and C. Helma, "Statistical evaluation of the predictive toxicology challenge 2000–2001," *Bioinformatics*, vol. 19, no. 10, pp. 1183–1193, 2003.
- [53] A. K. Debnath, R. L. Lopez de Compadre, G. Debnath, A. J. Shusterman, and C. Hansch, "Structure-activity relationship of mutagenic aromatic and heteroaromatic nitro compounds. correlation with molecular orbital energies and hydrophobicity," *Journal of medicinal chemistry*, vol. 34, no. 2, pp. 786–797, 1991.
- [54] P. Yanardag and S. Vishwanathan, "Deep graph kernels," in *Proceedings of the 21th ACM SIGKDD international conference on knowledge discovery and data mining*, 2015, pp. 1365–1374.
- [55] N. Shervashidze, S. Vishwanathan, T. Petri, K. Mehlhorn, and K. Borgwardt, "Efficient graphlet kernels for large graph comparison," in *Artificial Intelligence and Statistics*, 2009, pp. 488–495.
- [56] N. Shervashidze, P. Schweitzer, E. J. Van Leeuwen, K. Mehlhorn, and K. M. Borgwardt, "Weisfeiler-lehman graph kernels," *Journal of Machine Learning Research*, vol. 12, no. 9, 2011.
- [57] M. Zhang, Z. Cui, M. Neumann, and Y. Chen, "An end-to-end deep learning architecture for graph classification," in *Proceedings of the AAAI Conference on Artificial Intelligence*, vol. 32, no. 1, 2018.
- [58] K. Xu, W. Hu, J. Leskovec, and S. Jegelka, "How powerful are graph neural networks?" in *International Conference on Learning Representations*, 2018.
- [59] W. Zhao, Y. Fang, Z. Cui, T. Zhang, J. Yang, and W. Liu, "Graph deformer network," in *Proceedings of the Thirtieth International Joint Conference on Artificial Intelligence*, 2020, p. 1646–1652.
- [60] F.-Y. Sun, J. Hoffman, V. Verma, and J. Tang, "Infograph: Unsupervised and semi-supervised graph-level representation learning via mutual information maximization," in *International Conference on Learning Representations*, 2020.